Supporting Information (SI)

Nanostructured Carbons Containing FeNi/NiFe$_2$O$_4$ Supported Over N-doped Carbon Nanofibers for Oxygen Reduction and Evolution Reactions

Experimental Procedures

Electron transfer number 'n'

The electron transfer number (n) of the catalyst was calculated from the slope of Koutechy-Levich plot using the equation:

$$\frac{1}{j} = \frac{1}{j_k} + \frac{1}{B\omega^{1/2}}$$

Where j is the disk current density, j_k is the kinetic current density, ω is the electrode rotating speed, and B is expressed by:

$$B = 0.2nF(D_{O_2})^{2/3}\vartheta^{-1/6}C_{O_2}$$

Here, 0.2 is the rotation speed expressed in rpm, F is the Faraday constant (96,485 C mol^{-1}), D_{O_2} is the diffusion coefficient of O_2 in 0.1 M KOH (1.9 x 10^{-5} cm^2 s^{-1}), ϑ is the kinematic viscosity of the KOH solution (0.01 cm^2 s^{-1}), and C_{O_2} is the dissolved O_2 concentration (1.2 x 10^{-6} mol cm^{-3}). In the case of RRDE measurement, the ring current (i_R) and disk current (i_D) were collected using a Pt ring-disk electrode in O_2-saturated 0.1 M KOH (or 0.5 M H_2SO_4) solution at a rotating speed of 1600 rpm with a sweep rate of 10 mV s^{-1}. The Pt ring electrode was polarized at 0.5 V in 0.1 KOH electrolyte. The peroxide (H_2O_2) yield was determined by the following equations:

$$\%\, H_2O_2 = 200 \times \frac{i_R/N}{i_D + i_R/N}$$

Where N is the collection efficiency of the Pt ring electrode with a value of 0.37.

ECSA calculation

ECSAs of G/CNT@NCNF, GS@NCNF were calculated by using double layer capacitance (C_{DL}). C_{DL} can be found from the slope of plot between different scan rate and current density at potential of 1.003 V vs. RHE. The potential range chosen was 0.92-1.08 V vs. RHE where there is no apparent Faradic processes taking place and the current detected can be assigned to the double layer charging. The CV was scanned in 1M KOH at scan rates of 20, 30, 40, 50, 60 and 70 mV s^{-1}. The relationship between the double layer charging current and I and the electrochemical double layer capacitance C_{DL} is following.

$$i = vC_{DL}$$

Where v is the scan rate. The resulting difference between the anodic and cathodic charging current densities centered at 1.0 V versus RHE $\Delta J = (\frac{J_a - J_C}{2})$ is plotted against the scan rate. Which is expected to be a straight line and the slope of the plot gives C_{DL} value. By using the following relationship the ECSA can be calculated.

$$ECSA = C_{DL}/C_s$$

Where Cs is the specific capacitance of a sample under the specific condition of electrolyte and CDL is the double layer capacitance in the non-faradic region of the voltammogram. For FeNi the reported value of Cs is around 40 μF in alkaline conditions.

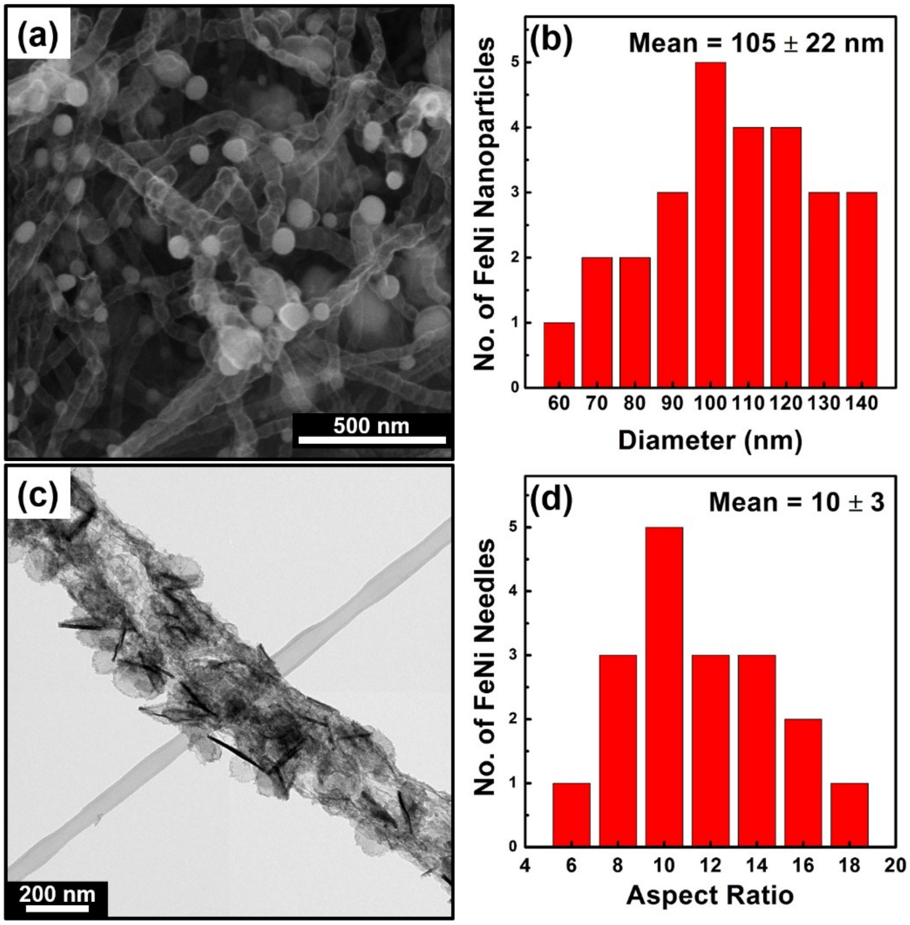

Figure S1. (a) SEM image of G/CNT@NCNF and (b) Particle size distribution of FeNi NPs located at the tips of the CNTs. (c) TEM image of GS@NCNF and (d) Aspect ratio distribution of needle-like FeNi.

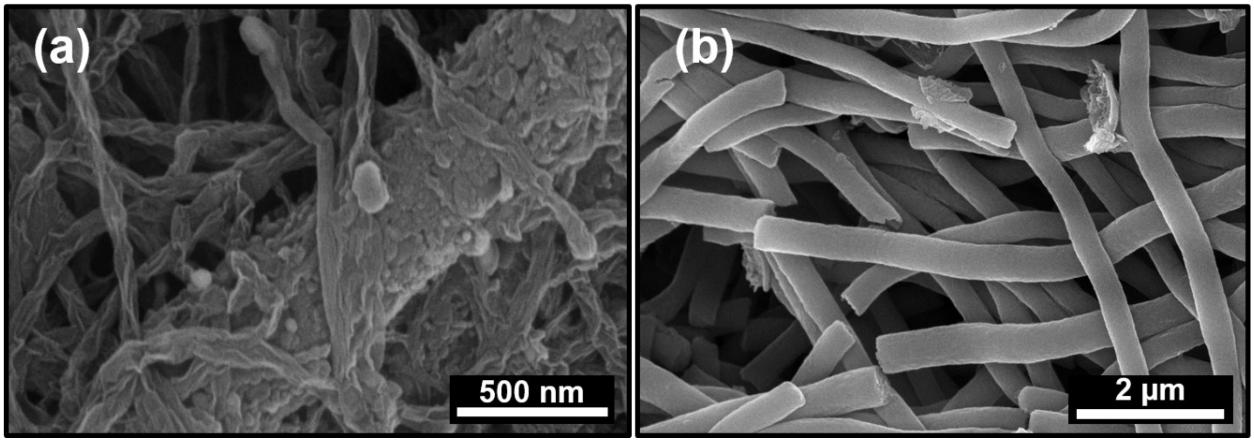

Figure S2. SEM image of (a) AT-G/CNT@NCNF and (b) AT-GS@NCNF samples.

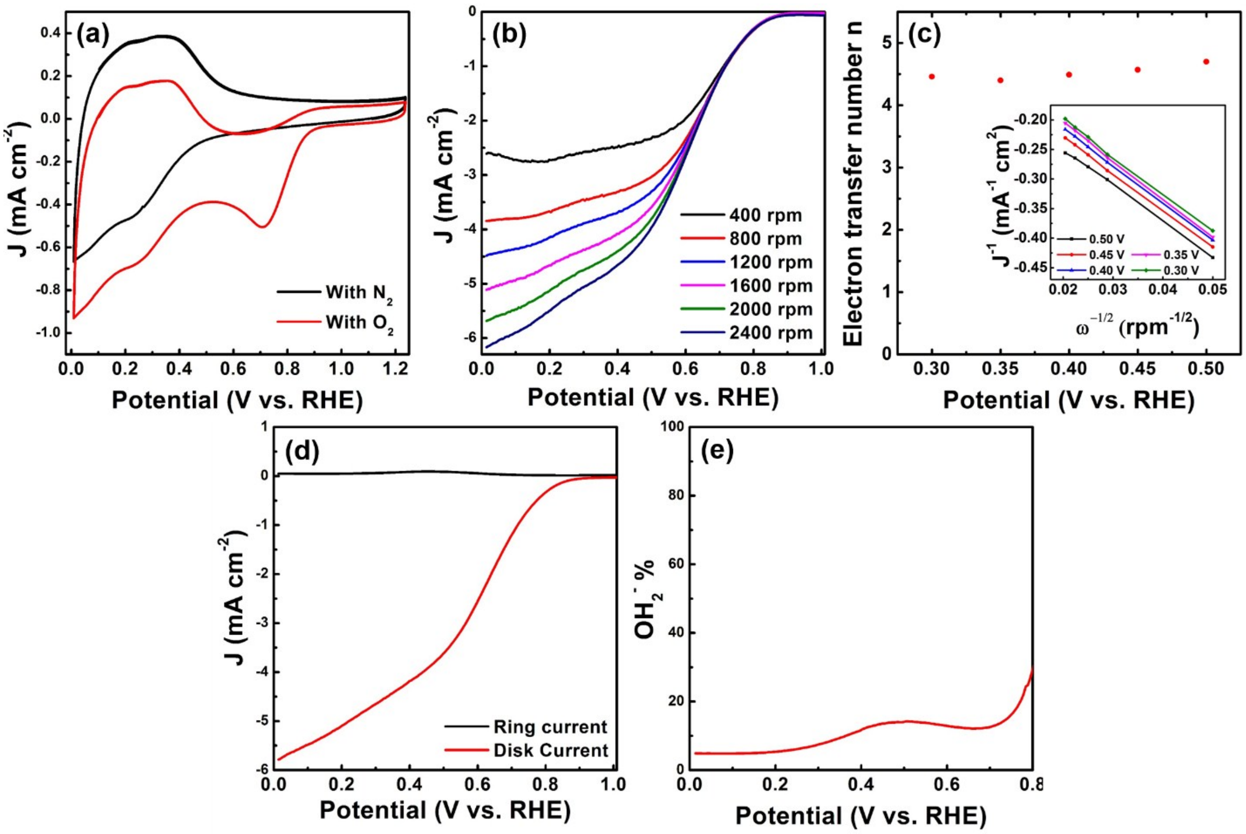

Figure S3. Catalytic activity towards ORR in 0.1 M KOH solution. (a) CVs of GS@NCNF in an O_2 and N_2-saturated KOH solution at a scan rate of 10 mV s^{-1}. (b) LSVs obtained for GS@NCNF at various speeds. (c) Electron transfer number 'n' and corresponding K-L plots (inset) of the GS@NCNF. (d) RRDE voltammograms in O_2-saturated KOH for the GS@NCNF at 1600 rpm and 10 mV s^{-1} where the ring electrode was polarized at 0.5 V. (e) Peroxide percentage as a function of electrode potential at 1600 rpm.

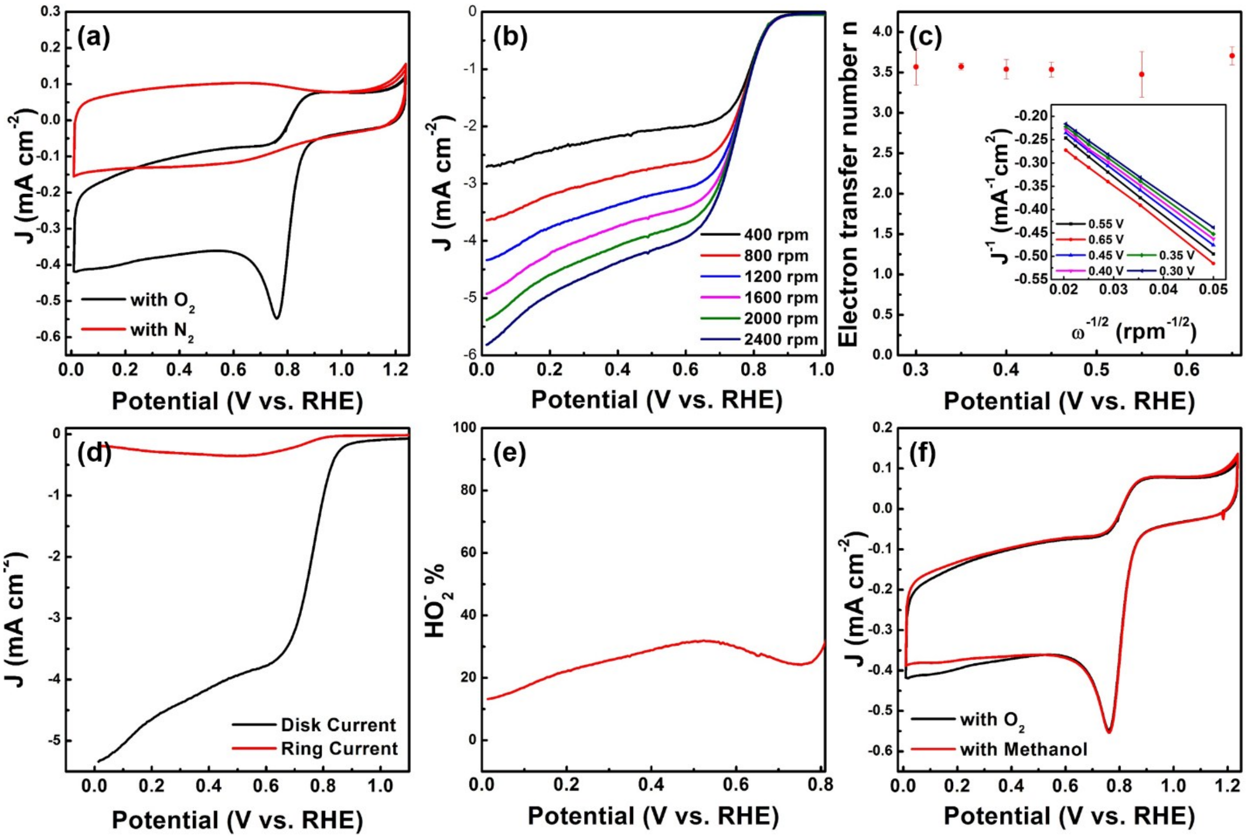

Figure S4. Catalytic activity towards ORR in 0.1 M KOH solution. (a) CVs of AT-G/CNT@NCNF in an O_2 and N_2-saturated KOH solution at a scan rate of 10 mV s^{-1}. (b) LSVs obtained for AT-G/CNT@NCNF at various rotating speeds. (c) Electron transfer number 'n' and corresponding K-L plots (inset) of the AT-G/CNT@NCNF. (d) RRDE voltammograms in O_2-saturated KOH for the AT-G/CNT@NCNF at 1600 rpm and 10 mV s^{-1} where the ring electrode was polarized at 0.5 V. (e) Peroxide percentage as a function of electrode potential at 1600 rpm. (f) CV of AT-G/CNT@NCNF in O_2-saturated 0.1 M KOH with and without 10 vol. % methanol at a scan rate of 10 mV s^{-1}.

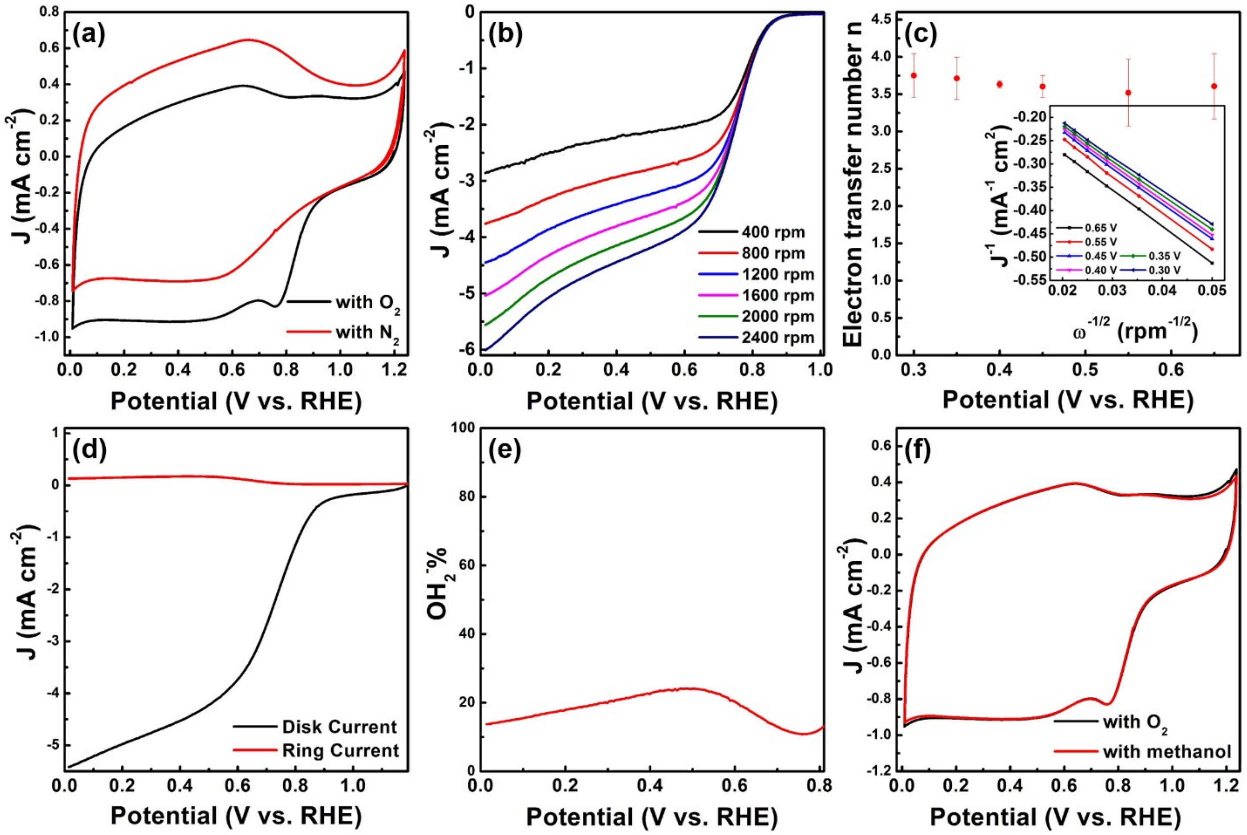

Figure S5. Catalytic activity towards ORR in 0.1 M KOH solution. (a) CVs of AT-GS@NCNF in an O_2 and N_2-saturated KOH solution at a scan rate of 10 mV s^{-1}. (b) LSVs obtained for AT-GS@NCNF at various rotating speeds. (c) Electron transfer number 'n' and corresponding K-L plots (inset) of the AT-GS@NCNF. (d) RRDE voltammograms in O_2-saturated KOH for the AT-GS@NCNF at 1600 rpm and 10 mV s^{-1} where the ring electrode was polarized at 0.5 V. (e) Peroxide percentage as a function of electrode potential at 1600 rpm. (f) CV of AT-GS@NCNF in O_2-saturated 0.1 M KOH with and without 10 vol. % methanol at a scan rate of 10 mV s^{-1}.

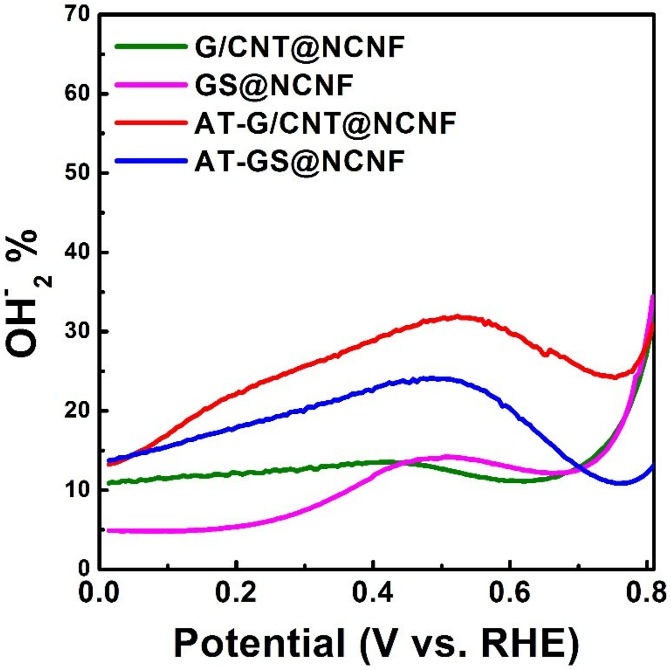

Figure S6. Comparison of H_2O_2 production of all the as-synthesized and acid treated catalysts.

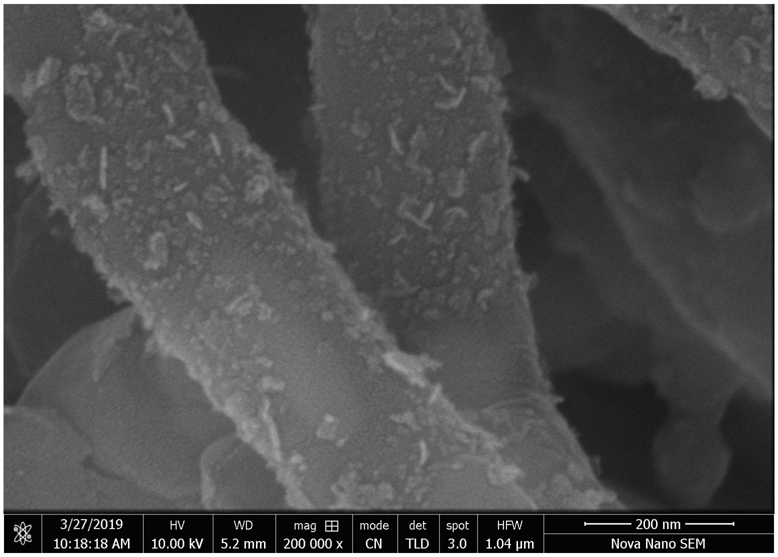

Figure S7. SEM image of AT-GS@NCNF after chronopotentiometry (4 h) showing structural damage.

Table S1. Onset potential, half wave potential and current density at 0.4 V for ORR and onset potential (@10 mAcm^{-2}) for OER with corresponding ΔE values.

Sample name	**ORR**			**OER** E_{onset} **(V)** **(10 mA cm^{-2})**	**ΔE= E** $_{OER\ (j=10)}$**-** $E_{1/2(ORR)}$ **V**
	E_{onset} **(V)**	$E_{1/2}$ **(V)**	**J @ 0.4V (mA cm^{-2})**		
Pt/C (40%)	1.01	0.79	-4.27	-	-
G/CNT@NCNF	0.948	0.74	-4.27	1.52	0.78
AT-G/CNT@NCNF	0.928	0.76	-3.73	1.55	0.79
GS@NCNF	0.850	0.63	-4.086	1.46	0.83
AT-GS@NCNF	0.928	0.76	-3.79	0	-

Table S2. Comparison of ORR performance in alkaline media for G/CNT@NCNF and GS@NCNF compared to similar materials in literature

Sample	E_{onset} **(V vs. RHE)**	$E_{1/2}$ **(V vs. RHE)**	$J_{0.4\ V}$ **(mA cm^{-2})**	**Loading amount (mg cm^{-2})**	**Ref.**
G/CNT@NCNF	0.948	0.74	4.27	0.400	This work
GS@NCNF	0.85	0.63	4.08	0.400	This work
Fe1Ni1-N-CNF	0.903	0.791	3.803	0.229	[1]
NiFe@NBCNT	1.08	0.83	-	0.2	[2]
N-CC@CNTs	-	0.88	-	0.09	[3]
CoNCNTF/CNF	0.974	0.857	-	0.4	[4]
FeNi@NCNTs/CC	0.95	0.77	4.7	1	[5]
NPCN/CoNi-NCNT	0.94	0.87	6	0.714	[6]

Table S3. Comparison of OER performance in alkaline media for G/CNT@NCNF and GS@NCNF compared to similar materials in literature.

Sample	Electrolyte	Potential at 10 mA cm^{-2} (V vs. RHE)	Tafel Slope (mV dec^{-1})	Reference
G/CNT@NCNF	1M KOH	1.52	51.5	This Work
GS@NCNF	1M KOH	1.46	97.9	This Work
Fe1Ni1-N-CNFs	0.1M KOH	1.60	106.1	[1]
FeNi/NiFe$_2$O$_4$@NC	1M KOH	1.54	60	[7]
CoNCNTF/CNF	0.1M KOH	1.61	66.8	[4]
NiCoO$_2$/CNTs	0.1M KOH	1.66	156	[8]
NiFe@NBCNT	1M KOH	1.425	79	[2]
FeNi@NCNTs/CC	1M KOH	1.48	142	[5]
NPCN/CoNi-NCNT	0.1M KOH	1.59	165	[6]

References:

(1) Wang, Z.; Li, M.; Fan, L.; Han, J.; Xiong, Y. Fe/Ni-N-CNFs electrochemical catalyst for oxygen reduction reaction/oxygen evolution reaction in alkaline media. *Appl. Surf. Sci.* **2017**, *401*, 89–99.

(2) Bin, D., Yang, B., Li, C., Liu, Y., Zhang, X., Wang, Y., & Xia, Y. In Situ Growth of NiFe Alloy Nanoparticles Embedded Into N-doped Bamboo-Like Carbon Nanotube as a Bifunctional Electrocatalyst for Zn- Air Battery. *ACS Appl. Mater. Interf.* **2018**, *10* (31), 26178–26187.

(3) Hu, C.; Wang, L.; Zhao, Y.; Ye, M.; Chen, Q.; Feng, Z.; Qu, L. Designing nitrogen-enriched echinus-like carbon capsules for highly efficient oxygen reduction reaction and lithium ion storage. *Nanoscale* **2014**, *6* (14), 8002–8009.

(4) Fan, L.; Ji, D.; Fan, L.; Li, L.; Mao, N.; Qin, X.; Peng, S. Hierarchical catalytic electrodes of cobalt-embedded carbon nanotube / carbon flakes array for flexible solid-state zinc-air batteries Hierarchical catalytic electrodes of cobalt-embedded carbon nanotube / carbon fl akes array for fl exible solid-state zinc-air batteries. *Carbon N. Y.* **2018**, *142* (October), 379–387.

(5) Zhao, X.; Abbas, S. C.; Huang, Y.; Lv, J.; Wu, M.; Wang, Y. Robust and Highly Active FeNi @ NCNT Nanowire Arrays as Integrated Air Electrode for Flexible Solid-State Rechargeable Zn-Air Batteries. **2018**, *1701448*, 1–7.

(6) Hou, Y.; Cui, S.; Wen, Z.; Guo, X.; Feng, X. Strongly Coupled 3D Hybrids of N-doped Porous Carbon Nanosheet / CoNi Alloy-Encapsulated Carbon Nanotubes for Enhanced

Electrocatalysis. **2015**, No. 44, 5940–5948.

(7) Dai, X.; Liu, M.; Yong, J.; Qiao, H.; Jin, A.; Li, Z.; Huang, X.; Wang, H.; Zhang, X. Strongly Coupled FeNi Alloys/NiFe2O4@Carbonitride Layers- Assembled Microboxes for Enhanced Oxygen Evolution Reaction. *ACS Appl. Mater. Interf.* **2016**, *8* (50), 34396–34404.

(8) Ma, L.; Zhou, H.; Sun, Y.; Xin, S.; Xiao, C.; Kumatani, A.; Matsue, T.; Zhang, P.; Ding, S.; Li, F. Nanosheet-structured NiCoO 2 / carbon nanotubes hybrid composite as a novel bifunctional oxygen electrocatalyst. *Electrochim. Acta* **2017**, *252*, 338–349.